J|A|C|S
ARTICLES
Published on Web 04/20/2002

An Ultrahigh Resolution Structure of TEM-1 β-Lactamase Suggests a Role for Glu166 as the General Base in Acylation

George Minasov, Xiaojun Wang, and Brian K. Shoichet*

Contribution from the Department of Molecular Pharmacology & Biological Chemistry, Northwestern University, 303 East Chicago Avenue, Chicago, Illinois 60611-3008

Received February 18, 2002

Abstract: Although TEM-1 β-lactamase is among the best studied enzymes, its acylation mechanism remains controversial. To investigate this problem, the structure of TEM-1 in complex with an acylation transition-state analogue was determined at ultrahigh resolution (0.85 Å) by X-ray crystallography. The quality of the data was such as to allow for refinement to an *R*-factor of 9.1% and an R_{free} of 11.2%. In the resulting structure, the electron density features were clear enough to differentiate between single and double bonds in carboxylate groups, to identify multiple conformations that are occupied by residues and loops, and to assign 70% of the protons in the protein. Unexpectedly, even at pH 8.0 where the protein was crystallized, the active site residue Glu166 is clearly protonated. This supports the hypothesis that Glu166 is the general base in the acylation half of the reaction cycle. This structure suggests that Glu166 acts through the catalytic water to activate Ser70 for nucleophilic attack on the β-lactam ring of the substrate. The hydrolytic mechanism of class A β-lactamases, such as TEM-1, appears to be symmetrical, as are the serine proteases. Apart from its mechanistic implications, this atomic resolution structure affords an unusually detailed view of the structure, dynamics, and hydrogen-bonding networks of TEM-1, which may be useful for the design of inhibitors against this key antibiotic resistance target.

Class A β-lactamases are the predominate source of bacterial resistance to the β-lactam family of antibiotics, such as the penicillins and the cephalosporins.[1] Consequently, these enzymes are targets for anti-resistance drug design[2,3] and have been extensively studied mechanistically since the seminal studies of Knowles.[4]

Among the best studied and most widespread of the class A β-lactamases is TEM-1, whose catalytic mechanism,[5−14] three-dimensional structure,[2,3,15−19] and potential for inhibition have drawn considerable attention.[2,3,19] TEM-1 catalyzes the hydrolysis of β-lactams near the diffusion limit (10^8 M^{-1} sec^{-1}) and is considered a "perfect enzyme".[11] It uses an active site serine nucleophile to cleave the lactam bond of the antibiotics, which inactivates them, in a mechanism that loosely resembles that of serine proteases.[20] The reaction begins with the formation of a precovalent encounter complex (Figure 1A), and moves through a high-energy acylation tetrahedral intermediate (Figure 1B) to form a transiently stable acyl-enzyme intermediate, forming an ester through the catalytic residue Ser70 (Figure 1C). Subsequently, the acyl-enzyme is attacked by a hydrolytic water (Figure 1D) to form a high-energy deacylation intermediate (Figure 1E), which collapses to form the hydrolyzed product (Figure 1F). The product is then expelled, regenerating free enzyme. As in serine proteases, this mechanism requires a catalytic base to activate the serine nucleophile to attack the amide bond of the substrate and, following formation of the acyl-enzyme, to activate the hydrolytic water for attack on the ester center of the adduct (Figure 1).

Whereas there is a consensus on the deacylation portion of the mechanism, the acylation part of the reaction has remained controversial. The key residue implicated in deacylation is believed to be the conserved Glu166, which is located on the catalytically critical Omega loop. Previous crystallographic studies suggested that the deacylation water is activated by the

* To whom correspondence should be addressed. E-mail: b-shoichet@northwestern.edu. Phone: 312-503-0081. Fax: 312-503-5349.

(1) Frere, J. M. *Mol. Microbiol.* **1995**, *16*, 385−95.
(2) Strynadka, N. C.; Martin, R.; Jensen, S. E.; Gold, M.; Jones, J. B. *Nat. Struct. Biol.* **1996**, *3*, 688−95.
(3) Ness, S.; Martin, R.; Kindler, A. M.; Paetzel, M.; Gold, M.; Jensen, S. E.; Jones, J. B.; Strynadka, N. C. *Biochemistry* **2000**, *39*, 5312−21.
(4) Knowles, J. R. *Acc. Chem. Res.* **1985**, *18*, 97−104.
(5) Delaire, M.; Lenfant, F.; Labia, R.; Masson, J. M. *Protein Eng.* **1991**, *4*, 805−10.
(6) Escobar, W. A.; Tan, A. K.; Lewis, E. R.; Fink, A. L. *Biochemistry* **1994**, *33*, 7619−26.
(7) Escobar, W. A.; Tan, A. K.; Fink, A. L. *Biochemistry* **1991**, *30*, 10783−7.
(8) Jacob, F.; Joris, B.; Lepage, S.; Dusart, J.; Frere, J. M. *Biochem. J.* **1990**, *271*, 399−406.
(9) Lietz, E. J.; Truher, H.; Kahn, D.; Hokenson, M. J.; Fink, A. L. *Biochemistry* **2000**, *39*, 4971−81.
(10) Damblon, C.; Raquet, X.; Lian, L. Y.; Lamotte-Brasseur, J.; Fonze, E.; Charlier, P.; Roberts, G. C.; Frere, J. M. *Proc. Natl. Acad. Sci. U.S.A.* **1996**, *93*, 1747−52.
(11) Martin, M. T.; Waley, S. G. *Biochem. J.* **1988**, *254*, 923−5.
(12) Christensen, H.; Martin, M. T.; Waley, S. G. *Biochem. J.* **1990**, *266*, 853−61.
(13) Massova, I.; Mobashery, S. *Curr. Pharm. Des.* **1999**, *5*, 929−37.
(14) Matagne, A.; Lamotte-Brasseur, J.; Dive, G.; Knox, J. R.; Frere, J. M. *Biochem. J.* **1993**, *293*, 607−11.
(15) Herzberg, O. *J. Mol. Biol.* **1991**, *217*, 701−19.
(16) Herzberg, O.; Moult, J. *Science* **1987**, *236*, 694−701.
(17) Dideberg, O.; Charlier, P.; Wery, J. P.; Dehottay, P.; Dusart, J.; Erpicum, T.; Frere, J. M.; Ghuysen, J. M. *Biochem. J.* **1987**, *245*, 911−3.
(18) Chen, C. C.; Smith, T. J.; Kapadia, G.; Wasch, S.; Zawadzke, L. E.; Coulson, A.; Herzberg, O. *Biochemistry* **1996**, *35*, 12251−8.
(19) Rahil, J.; Pratt, R. F. *Biochemistry* **1994**, *33*, 116−25.
(20) Lamotte-Brasseur, J.; Dive, G.; Dideberg, O.; Charlier, P.; Frere, J. M.; Ghuysen, J. M. *Biochem. J.* **1991**, *279*, 213−21.

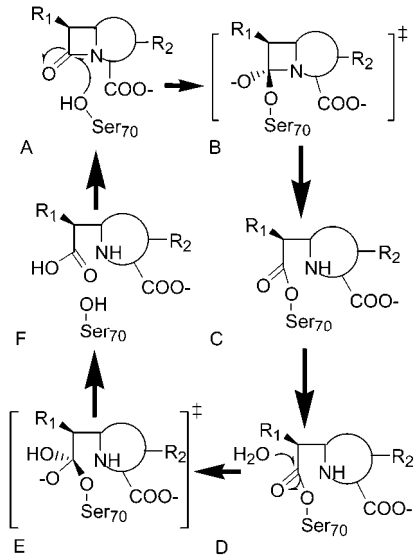

Figure 1. The reaction cycle of TEM-1 β-lactamase. The two states in braces represent the acylation and deacylation tetrahedral high-energy intermediates.

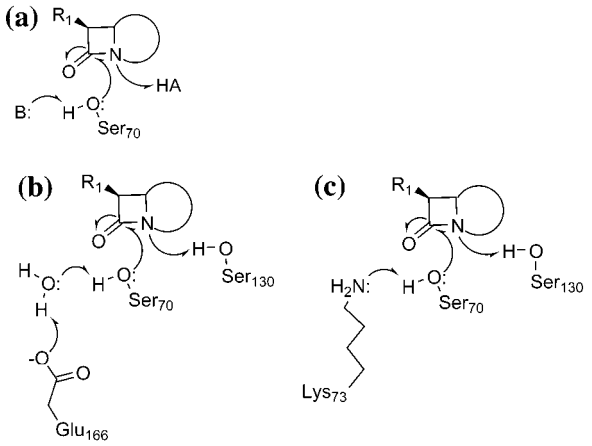

Figure 2. Two candidate mechanisms for acylation of TEM-1 β-lactamase.[2,9,10,16,20,21,23,24] (A) Nucleophilic attack of Ser70 Oγ on the lactam carbonyl carbon. (B) Proposed role of Glu166 as the catalytic base in acylation. (C) Proposed role of Lys73 as the catalytic base in acylation.

carboxylate of Glu166, which plays the role of the catalytic base in deacylation.[16,21] This view is consistent with site-directed mutagenesis studies[22] and the structural determination of complexes between TEM-1 and deacylation transition-state analogues.[2,3] On the other hand, two mechanisms have been mooted for the formation of the acyl-enzyme adduct (Figure 2A). In one mechanism, the catalytically key residue Lys73 is proposed to be the catalytic base in its deprotonated state, activating Ser70 for attack on the lactam carbonyl carbon[2,16,21,23] (Figure 2C). This would result in an asymmetrical hydrolytic mechanism. In the second mechanism, Glu166 would play the role of the catalytic base in acylation, activating Ser70 mediated through a bound water (Figure 2B).[9,10,20,24] Despite extensive site-directed mutagenesis studies[5−7,9,18,23,25,26] and structural investigations by both X-ray crystallography and NMR,[2,10,19,21,22,24,27] no consensus has emerged that favors one mechanism over the other.

The Lys73 hypothesis (Figure 2C) is supported by site-directed mutagenesis and structural studies. When class A β-lactamases are substituted at this residue, which is completely conserved,[28] catalytic activity drops by 10^3-fold or more against penicillins.[9,18,25] This suggests that Lys73 plays a direct[18,25] or indirect[9] role in acylation and deacylation. In several class A β-lactamase structures, the Nζ atom of Lys73 appears to hydrogen bond to Ser70 Oγ, consistent with a role as the general base activating Ser70 for nucleophilic attack.[2,21,27] Although substitutions at the completely conserved Glu166 also resulted in 10^2 to 10^5-fold reduction in activity,[6,7,23,25,26] two lines of evidence seem to favor the Lys73 hypothesis: (1) the acylation rate was less affected than the deacylation rate by substitutions at Glu166; and (2) it was possible to trap acyl-enzyme intermediates of β-lactams bound to these mutants.[7,21,23,26,29] The simplest explanation of these data was that Lys73 acts as the general base in acylation and Glu166 acts in deacylation,[25] although alternative explanations have been proposed (where Lys73 is only important in proton shuttling in both states).[9]

On the other hand, the Glu166 hypothesis (Figure 2B) is supported by activity studies of the pH dependence for wild type (WT), Lys73 mutants and Glu166 mutants.[5,6,9] In WT enzyme, the pH dependence of the acylation rate constant is a bell-shaped, with a pK_{a1} of 5.0 and pK_{a2} of 8.5. The acidic limb pK_a is widely thought to represent the protonation state of Glu166.[5,6,30] The origin of the basic limb pK_a remains controversial.[5,6,9] Whereas the mutant K73A activity retained bell-shaped pH dependence, with higher pK_{a1} 8.0 and pK_{a2} 8.9,[9] the charge-neutral mutant enzymes E166Y and E166C had sigmoidal pH-dependence curves with a single pK_a above 8.0.[5,6] In addition, Waley and colleagues showed that acylation and deacylation constants have the same pH profile.[11] These data suggest that Glu166 plays a role as a general base in acylation. Additionally, for Lys73 to act as a catalytic base, it would have to be deprotonated at physiological pH (Figure 2). However, NMR evidence suggests that the pK_a of this residue is greater than 10,[10] which seems inconsistent with the Lys73 hypothesis. Finally, X-ray crystallographic evidence, which has been used to support a role for Lys73 as the catalytic base, is also consistent with a role for Glu166, which is observed to hydrogen bond to the catalytic water (Wat1004 in this study) that, in turn, is observed to hydrogen bond with the nucleophilic Ser70.

An issue with the X-ray crystallographic studies is that they have not been conducted at a resolution high enough to determine the protonation states of Lys73 and Glu166, which is crucial to analyzing their roles as catalytic bases. Here we describe the structure of TEM-1 β-lactamase in complex with an acylation transition-state analogue (Table 2) at 0.85 Å. This

(21) Strynadka, N. C.; Adachi, H.; Jensen, S. E.; Johns, K.; Sielecki, A.; Betzel, C.; Sutoh, K.; James, M. N. *Nature* **1992**, *359*, 700−5.
(22) Madgwick, P. J.; Waley, S. G. *Biochem. J.* **1987**, *248*, 657−62.
(23) Leung, Y. C.; Robinson, C. V.; Aplin, R. T.; Waley, S. G. *Biochem. J.* **1994**, *299*, 671−8.
(24) Mustafi, D.; Sosa-Peinado, A.; Makinen, M. W. *Biochemistry* **2001**, *40*, 2397−409.
(25) Gibson, R. M.; Christensen, H.; Waley, S. G. *Biochem. J.* **1990**, *272*, 613−9.
(26) Adachi, H.; Ohta, T.; Matsuzawa, H. *J. Biol. Chem.* **1991**, *266*, 3186−91.
(27) Maveyraud, L.; Pratt, R. F.; Samama, J. P. *Biochemistry* **1998**, *37*, 2622−8.
(28) Joris, B.; Ghuysen, J. M.; Dive, G.; Renard, A.; Dideberg, O.; Charlier, P.; Frere, J. M.; Kelly, J. A.; Boyington, J. C.; Moews, P. C.; et al. *Biochem. J.* **1988**, *250*, 313−24.
(29) Chen, C. C.; Herzberg, O. *Biochemistry* **2001**, *40*, 2351−8.
(30) Ellerby, L. M.; Escobar, W. A.; Fink, A. L.; Mitchinson, C.; Wells, J. A. *Biochemistry* **1990**, *29*, 5797−806.

Table 1. Data and Refinement Statistics

	M182T/compound **1**
unit cell parameters (Å)	$a = 41.31$, $b = 61.64$, $c = 89.25$
resolution (Å)	15.0−0.85 (0.87−0.85)[a]
unique reflections	200 302 (13 237)
total observations	1 143 489
R_{merge} (%)	5.2 (42.0)
completeness (%)	100.0 (100.0)
$\langle I \rangle / \langle \sigma(I) \rangle$	25.7 (3.8)
number of protein residues	263
number of ions	3 HPO_4^{2-}, 4 K^+
number of water molecules	566
rmsd bond lengths (Å)	0.014
rmsd angles (deg)	2.6
R-factor	9.10
R_{free}	11.17

[a] Values in parentheses are for the highest resolution shell.

ultrahigh-resolution structure allows us to observe the protonation state of Lys73, Glu166, and Wat1004, and to determine the manner in which they interact with Ser70 and the transition-state analogue. This structure goes some ways toward resolving the question of the identity of the catalytic base in acylation and the overall flow of protons throughout the reaction pathway. Furthermore, the ability to place most protons in this structure and to resolve alternative conformations may help with inhibitor design studies against this key antibiotic resistance target.

Materials and Methods

Preparation of TEM-1 Mutant M182T. This work was conducted with a stabilized mutant TEM-1, M182T.[31] The substitution Met182 → Thr stabilizes the mutant enzyme by 2.6 kcal/mol relative to wild type (WT),[32] but has very little effect on catalytic activity;[31] the substitution is 15 Å from the catalytic serine, far from the active site. The mutant was prepared by a two-step PCR protocol.[33,34] In brief, two PCR reactions were performed: one involved a mutagenesis anti-sense primer and a sense primer that covered the *Nde*I site that flanks the 5′ end of the gene, and the second involved a sense mutagenesis primer and an anti-sense primer covering the *Eco*RI site that flanks the 3′ end of the gene. The reaction volume of 100 μL included 2.5 units of *Pfu* DNA polymerase (Stratagene), reaction buffer provided by Stratagene, 100 ng of pAlter Ex II TEM-1, 250 ng of flanking primer, 250 ng of mutagenesis primer, and each dNTP at 0.2 mM. The PCR products were purified with QIAquick Gel Extraction kit (Qiagen, Valencia, CA). In the second step, PCR was performed in the same buffer using 100 ng of each of the first-round products and 250 ng of each flanking primer. The PCR product was purified with QIAquick PCR Purification kit (Qiagen) and digested with *Nde*I and *Eco*RI. The digested product was again purified with QIAquick PCR Purification kit, subsequently ligated into pAlter Ex II TEM-1 plasmid predigested with *Nde*I and *Eco*RI and then transformed into JM109 cells. The modified pAlter Ex II TEM-1 was subsequently purified and sequenced to verify the mutation.

The mutated TEM-1 enzyme was expressed and purified in a procedure modified from Dubus et al.[34,35] The protein was expressed from cells growing at room temperature in 2xYT medium in a 2-L fermenter for 22 h. Cells were collected by centrifugation and resuspended in 5 mM Tris/HCl, pH 8.0, containing 1 mM EDTA and 20% (w/v) sucrose at room temperature for 10 min. Cells were then collected and resuspended in ice-cold 5 mM $MgCl_2$ for 10 min. The supernatant was saved as the periplasmic contents, concentrated to about 100 mL, and dialyzed against 5 mM Tris/HCl, pH 8.0. The crude extract was applied to a Q-Sepharose FF column (Pharmacia, Uppsala, Sweden) equilibrated with 5 mM Tris/HCl, pH 8.0. The column was then washed extensively with 5 mM Tris/HCl, pH 8.0. The enzyme was eluted by 5 mM Tris/HCl, pH 8.0, containing 100 mM NaCl. The active fractions were pooled and dialyzed against 100 mM sodium phosphate, pH 8.0. The enzyme solution was concentrated to 6 mg/mL and stored in 200 mM potassium phosphate, pH 7.0, 50% glycerol at −20 °C.

Crystallization and Data Collection. Crystals of the complex of TEM M182T with compound **1**, {[2-amino-α-(1-carboxyl-1-methyl-ethoxyimino)-4-thiazoleacetyl]amino}methaneboronic acid, which is a boronic acid transition state analogue inhibitor,[36] were grown by seeding techniques. An 8 μL droplet containing 5 mg/mL of the enzyme and 2.5 mM compound **1** in 0.65 M sodium−potassium phosphate buffer, pH 8.0, were seeded with microcrystals of apo M182T[32] and placed over 1.4 M sodium−potassium phosphate well buffer, pH 8.0. Single crystals appeared in 7 days and grew to a maximum size of 0.4 × 0.4 × 0.6 mm^3 in two weeks. Crystals were soaked in cryo-protectant (25% sucrose in 1.6 M phosphate buffer, pH 8.0) for 60 s and then frozen in liquid nitrogen. Diffraction data were collected from a single crystal on the 5ID beamline of the DND-CAT at Advanced Photon Source (Argonne, IL). Two sets of data, at high and low resolution, were collected at a wavelength of 0.7999 Å ($E = 15.5$ keV) using a MARCCD detector. A total of 484 frames were integrated, and 1 143 489 reflections were scaled and merged using DENZO/SCALEPACK package.[37] The data are 100% complete to 0.85 Å resolution (200 302 unique reflections, Table 1). Crystals belong to the space group $P2_12_12_1$ with unit cell parameters of 41.31, 61.64, and 89.25 Å, which are similar to the unit cell parameters of the M182T apo-enzyme crystals[32] and to those of WT.[21]

Refinement. Standard conjugate gradient refinement (CGLS) was carried out with SHELX97[38] using the apo-M182T structure[32] as an initial model. Three percent of the data (6015 reflections) was set aside randomly as the test set. The resolution was increased stepwise from 2.0 to 0.85 Å (Table 2). The model was manually corrected using $2F_o - F_c$ and $F_o - F_c$ σ_A-weighted maps displayed with TURBO[39] on a Silicon Graphics computer. Compound **1** was fit into unambiguous difference density. At this stage, about 60% of the residues was modeled in multiple conformations to interpret features of an $F_o - F_c$ electron density map (Table 2). The model was then refined using ADPs (anisotropic displacement parameters) with standard DELU (rigid-bond restraint), SIMU (restraint for spatially adjacent atoms), and ISOR (restraint for isolated atoms to be approximately isotropic) restraints, and converged at *R*-factor/R_{free} 10.9/13.0%. The introduction of all hydrogen atoms in the model lowered *R*-factors to 9.7/11.7% (Table 2). At this stage, DELU, SIMU, and ISOR restraints were adjusted using the program PARVATI.[40] In the final stage of refinement, torsion angle refinement was applied for hydrogen atoms of hydroxyl and methyl groups and "riding"[38] model refinement (constrained refinement of hydrogen atoms) for the rest. In the final model we kept only hydrogen atoms that gave positive 1.5σ level peaks in the $F_o - F_c$ hydrogen-omit density map. The final *R*-factors were 9.1% for *R*-factor and 11.2% for R_{free} (Table 2). In the final model, 169 of 263 total protein residues were modeled in multiple conformations.

Results

Ultrahigh-Resolution Features of TEM M182T. Most crystal structures of TEM-1 are determined at around 1.7 Å

(31) Huang, W.; Palzkill, T. *Proc. Natl. Acad. Sci. U.S.A.* **1997**, *94*, 8801−6.
(32) Wang, X.; Minasov, G.; Shoichet, B. K. *J. Mol. Biol.* **2002**, submitted for publication.
(33) Ho, S. N.; Hunt, H. D.; Horton, R. M.; Pullen, J. K.; Pease, L. R. *Gene* **1989**, *77*, 51−9.
(34) Wang, X.; Minasov, G.; Shoichet, B. K. *Protein* **2002**, *47*, 86−96.
(35) Dubus, A.; Wilkin, J. M.; Raquet, X.; Normark, S.; Frere, J. M. *Biochem. J.* **1994**, *301*, 485−94.
(36) Caselli, E.; Powers, R. A.; Blasczcak, L. C.; Wu, C. Y.; Prati, F.; Shoichet, B. K. *Chem. Biol.* **2001**, *8*, 17−31.
(37) Otwinowski, Z.; Minor, W. *Methods Enzymol.* **1997**, *276*, 307−326.
(38) Sheldrick, G. M.; Schneider, T. R. *Methods Enzymol.* **1997**, *277*, 319−343.
(39) Cambillau, C.; Roussel, A. *Turbo Frodo*, OpenGL ed.; Universite Aix-Marseille II: Marseille, France, 1997.
(40) Merritt, E. A. *Acta Crystallogr., Sect. D* **1999**, *55*, 1109−17.

Table 2. Progress of Refinement in SHELXL

step	action	residues with multiple conformations	hydrogen atoms	water/disordered water/ other	number of parameter	*R*-factor (%)	R_{free} (%)[a]
1	resolution to 1.2 Å	0	0	0/0/0	8111	27.90	31.69
2	ligand and water added	0	0	138/0/22	8663	22.51	25.33
3	more solvent	0	0	378/10/26	9767	17.71	21.58
4	resolution to 1.0 Å	0	0	378/10/26	9767	18.60	20.31
5	alternative conformations	53	0	409/72/35	11 945	16.35	18.77
6	resolution to 0.85 Å	53	0	409/72/35	11 945	18.04	18.82
7	more alternative conformations	154	0	357/186/36	15 221	16.06	17.74
8	anisotropicity applied	154	0	357/186/36	34 216	12.21	14.15
9	minor adjustments	155	0	435/252/52	35 679	10.92	13.02
10	hydrogen atoms added	155	2420	435/252/52	35 989	9.73	11.72
11	final model	169	1683	413/385/64	36 034	9.10	11.17

[a] R_{free} was calculated with 3% of reflections set aside randomly.

Table 3. Active Site Interactions Observed in the Compound **1** Complex with M182T

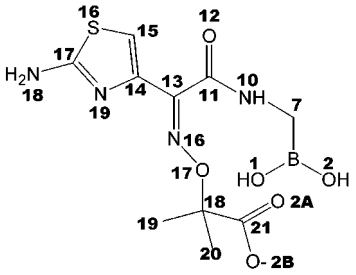

interactions	distance (Å)[a]	interactions	distance (Å)[a]
S70N−O1	2.9	S130Oδ−S70Oγ	3.1
A237N−O1	2.9	S130Oδ−K73Nζ	3.2
A237O−N10	3.4	K73Nζ−E166Oϵ2	3.6
A237O−O1	2.8	K73Nζ−S70Oγ	2.8
S130Oγ−O2	2.7	Wat 1004−E166Oϵ2	2.6
N132Nδ1−O12	2.9	Wat 1004−N170Oδ1	2.7
Wat 1076−O2	2.8	Wat 1004−S70Oγ	2.8
Wat 1076−N5	3.1	N132Oδ1−E166Oϵ2	3.1
E240Oϵ2−N18	3.0	N132Oδ1−K73Nζ	2.7
S130Oγ−K234Nζ	2.8	N170Nδ2−E166Oϵ1	2.8

[a] From distances measured only in one alternative conformation, which are within 0.1 Å for the other.

resolution. Here we report the crystal structure of a boronic acid (compound **1**,[36] Table 3) complex of the TEM-1 M182T mutant at 0.85 Å resolution, the highest resolution obtained for a β-lactamase and among the highest for any enzyme.[41−45] Among the factors that may contribute to the dramatic increase in resolution are the mutation M182T, which was shown to be an activity-neutral "global stabilizer",[31,32,46] the presence of the inhibitor, which had stabilizing effect on the enzyme, and data collection at a third-generation synchrotron radiation source.

The quality of the data and refinement are summarized in Tables 1 and 2. The slightly high R_{merge} in the last shell is due to high redundancy of the data. It was included in the refinement because the completeness of this shell was 100%, and the average $I/\sigma(I)$ for reflections in the shell was close to 4.0 (Table 1). The low *R*-factors for the test and the working sets indicate the high quality of the final model (Table 2). There is a dramatic increase in the quality and details of the electron density maps at this ultrahigh resolution. Individual atoms such as C, N, and O can be distinguished on the basis of the volume of the density. The shape of the density at single and double bonds is different in the carboxylate groups of glutamate and aspartate (Figure 3A). Thus, for Asp273 the electron density at the 2.0σ level for Oδ2 is discrete, while the density for Oδ1 is closer to and continuous between Cγ, which would be consistent with a single (longer) bond between Oδ2 and Cγ and a double bond between Oδ1 and Cγ (Figure 3A). For the sulfur atoms of Met69, density is consistent with the location of lone pair electrons, which are observed as positive peaks in $F_o - F_c$ map at 1.5σ (Figure 3B). Finally, difference density for more than 70% of all hydrogen atoms (1683/2420) was observed as peaks at the 1.5σ level. We chose this level as a cutoff for modeling a hydrogen atom into density, reasoning that a level of 3.0σ is typically used to assign heavy atom positioning into $F_o - F_c$ maps in lower resolution structures, thus making a 1.5σ cutoff for a hydrogen with only two electrons in its bonding orbital reasonable. The quality of the data allowed us to refine positions of the hydrogen atoms in methyl and hydroxyl groups using torsion angle refinement and to use the "riding"[38] model refinement for the rest of the hydrogen atoms in SHELXL. Figure 3C shows the electron density maps for the Thr180−Thr181−Thr182 region of the structure. Well-defined positive peaks at 2.0σ level in the $F_o - F_c$ density map are located near predicted hydrogen atoms. Peaks were found for all main-chain hydrogen atoms, except for several regions adopting multiple conformations, and for most side-chain hydrogen atoms. Surprisingly, it was even possible to assign proton positions to several water molecules that had unambiguous positive difference peaks (Figure 3D).

Hydrogen Atoms in the Active Site. The ultrahigh-resolution structure of TEM-1 β-lactamase provides a detailed picture of the hydrogen atoms in the active site. Unambiguous electron density in both $F_o - F_c$ and $2F_o - F_c$ maps suggested that the boronic acid transition-state analogue **1** (Table 3 and Figure 4A and D) is covalently bound to Oγ of Ser70, as expected. Both maps indicated that the side chain of compound **1**, which mimics the R1-sided chain of ceftazidime,[36] adopts two alternative conformations, involving a rotation around the Cβ−Oγ−B−C7 torsion angle (Figure 4A). One hydrogen atom is visible in $F_o - F_c$ density map at 1.4σ level, on the O2 atom of the boronic acid (Figure 4B). We note that the shape of the $2F_o - F_c$ density map suggested that the proton on the O1 oxygen of the boronic acid, corresponding to the position of the "oxyan-

(41) Teeter, M. M.; Roe, S. M.; Heo, N. H. *J. Mol. Biol.* **1993**, *230*, 292−311.
(42) Genick, U. K.; Soltis, S. M.; Kuhn, P.; Canestrelli, I. L.; Getzoff, E. D. *Nature* **1998**, *392*, 206−9.
(43) Kuhn, P.; Knapp, M.; Soltis, S. M.; Ganshaw, G.; Thoene, M.; Bott, R. *Biochemistry* **1998**, *37*, 13446−52.
(44) Rypniewski, W. R.; Ostergaard, P. R.; Norregaard-Madsen, M.; Dauter, M.; Wilson, K. S. *Acta Crystallogr., Sect. D* **2001**, *57*, 8−19.
(45) Jelsch, C.; Teeter, M. M.; Lamzin, V.; Pichon-Pesme, V.; Blessing, R. H.; Lecomte, C. *Proc. Natl. Acad. Sci. U.S.A.* **2000**, *97*, 3171−6.
(46) Sideraki, V.; Huang, W.; Palzkill, T.; Gilbert, H. F. *Proc. Natl. Acad. Sci. U.S.A.* **2001**, *98*, 283−8.

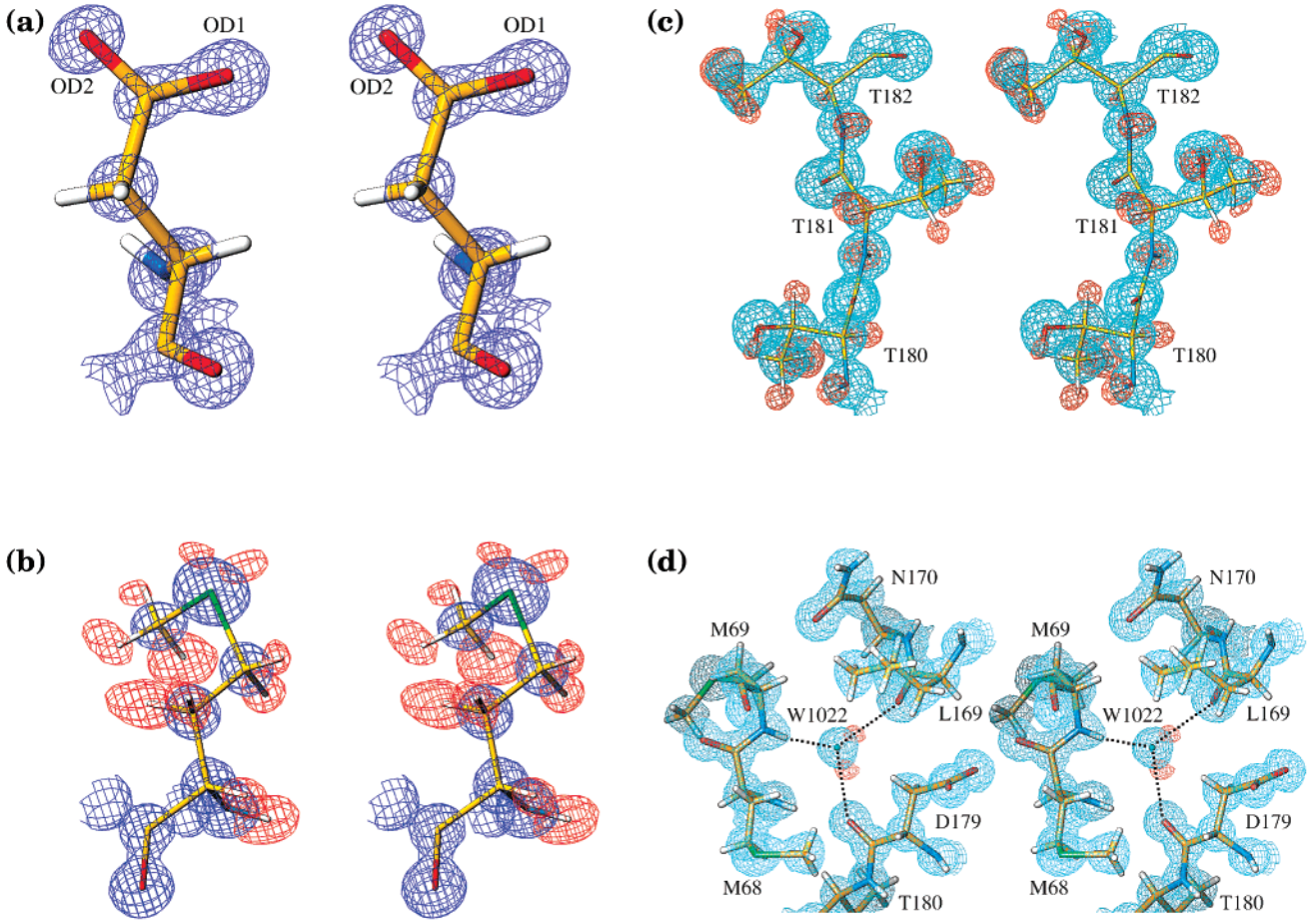

Figure 3. Quality of the electron density for the TEM-1 crystal structure at ultrahigh resolution. Residues in the region are labeled, and carbon, nitrogen, oxygen, sulfur, and hydrogen atoms in the model are colored in yellow, blue, red, green, and gray, respectively. (A) Stereoview of carboxylate group of Asp273 surrounded with $2F_o - F_c$ σ_A-weighted density map contoured at 2.0σ (blue). The double Oδ1−Cγ and single Oδ2−Cγ bonds can be easily distinguished. (B) Stereoview of Met69 surrounded with $2F_o - F_c$ σ_A-weighted density map contoured at 2.0σ (blue) and $F_o - F_c$ hydrogen-omit map contoured at 1.5σ (red). (C) Stereoview of Thr180−Thr182 region of the final model superimposed on $2F_o - F_c$ σ_A-weighted electron density map contoured at 1.0σ (cyan) and $F_o - F_c$ hydrogen-omit density map contoured at 2.0σ (red). (D) Stereoview of a water molecule in the final model with $2F_o - F_c$ σ_A-weighted density map in cyan (1.0σ) and two peaks of positive $F_o - F_c$ density in red (2.0σ) corresponding to hydrogen atoms on the water. Residues around the water are labeled, and hydrogen bonds are depicted as dashed lines.

ion"[47] or "hydroxyl",[48] is pointed toward the carbonyl oxygen of Ala237, consistent with earlier predictions. Nevertheless, we felt that the evidence for these proton positions was not strong enough to include those in the final model. In addition, hydrogen atoms were visible on C7, N10, and C15 of compound **1**. No hydrogen atoms were modeled for N18, C19, and C20 that are located at the end of compound **1**, due to the high B-factors of these atoms.

Most hydrogen atoms on the side-chain termini of Lys234, Ser130, Lys73, Asn170, Ala 237, and Asn132 are clearly visible at 1.5σ level (see Figure 4B for representative density). The Oδ1 and Oδ2 from Glu166 were unambiguously differentiated by their densities and had different bond lengths, consistent with one atom being predominantly double bonded and the other being predominantly single bonded in the asymmetric environment of the protein (Figure 4C). Unexpectedly, even at a pH 8.0 where the crystal was grown, strong positive density at Oϵ2 was present to indicate that Glu166 was protonated (Figure 4C and see below for detailed discussion). Peaks of positive difference density on the proposed deacylation water (WAT1004)[2,3] pointed toward Oδ1 of Asn170 (1.6 σ) and toward Oγ of Ser70 (1.4 σ), indicating unambiguous hydrogen atoms on this water (Figure 4C).

Discussion

Perhaps the most immediately interesting result to emerge from this structure is the protonation state of Glu166 and the subsequent hydrogen-bonding network in which it participates in a complex that mimics the high-energy acylation intermediate. In this complex, Glu166 appears to be protonated on the basis of strong difference density features (Figure 4C). This glutamic acid proton is donated to Wat1004 to form a hydrogen bond. This water, in turn, donates one of its protons to the catalytic Ser70, which, because it is forming an acyl-adduct with the transition-state analogue, can only accept a proton. That Glu166 should be protonated in this structure, even at pH 8.0, and that the key conserved Wat1004 should be positioned to accept this proton and donate its own proton to Ser70, seems compelling to us. An appealing interpretation of these observations is that Glu166, acting as the ultimate catalytic base for acylation, activates Wat1004, which, in turn, activates Ser70. This activation leads to a proton shuttle from the serine to the water to the glutamic acid.

(47) Murphy, B. P.; Pratt, R. F. *Biochem. J.* **1988**, *256*, 669−72.
(48) Usher, K. C.; Blaszczak, L. C.; Weston, G. S.; Shoichet, B. K.; Remington, S. J. *Biochemistry* **1998**, *37*, 16082−92.

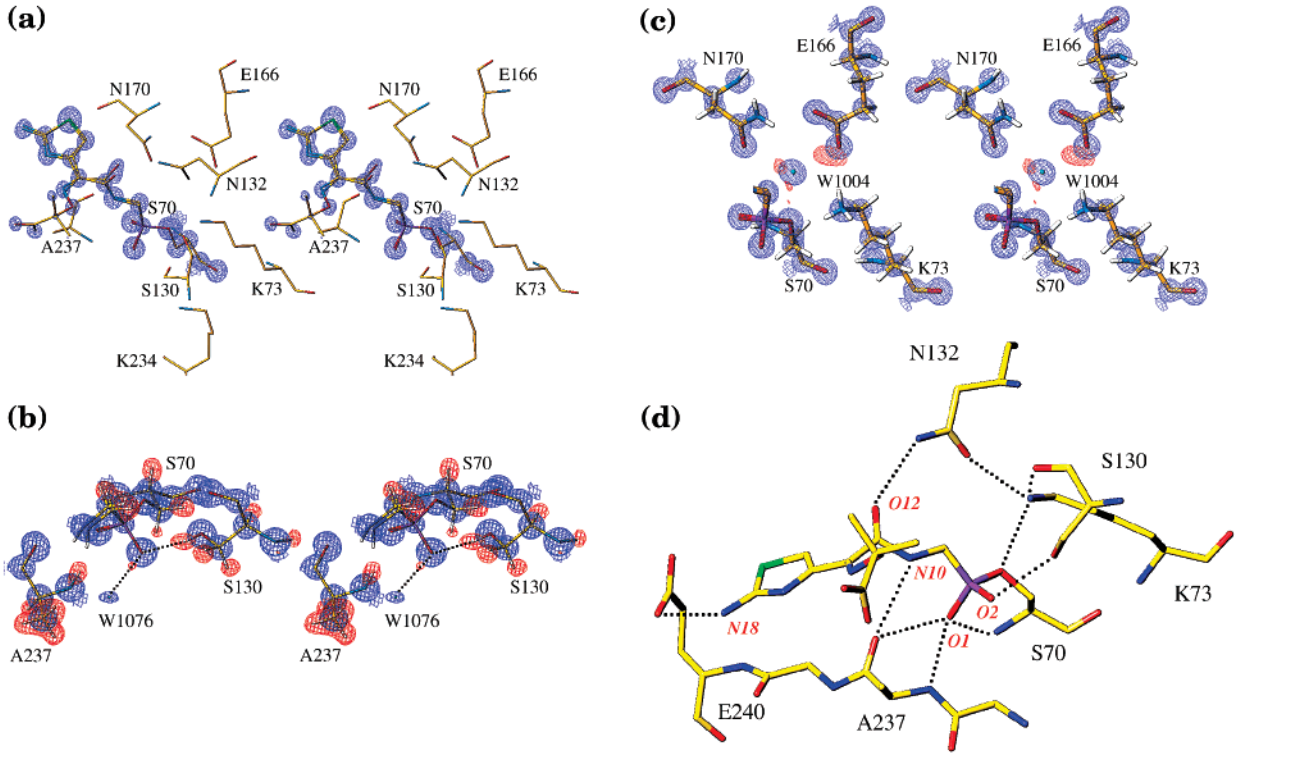

Figure 4. Electron density in the active site of TEM M182T at ultrahigh resolution. (A) Stereoview of compound **1** covalently bound to Ser70 surrounded with $2F_o - F_c$ σ_A-weighted density map contoured at 2.0σ. Selected conserved residues are colored as in Figure 3, except the boron atom in the model is colored in purple. (B) Stereoview of hydrogen atoms on the conserved residues of binding site superimposed on the $2F_o - F_c$ in blue (2.0σ) and $F_o - F_c$ in red (1.4σ) hydrogen-omit density map. The hydrogen of hydroxyl group of Ser130 is pointed to the oxygen (O2) of the boronate (see text for details). (C) Stereoview of the conserved water and selected residues of the active site surrounded with $2F_o - F_c$ in blue (2.0σ) and $F_o - F_c$ in red (1.4σ) σ_A-weighted density maps. The red peak at Oϵ2 of Glu166 indicates that the carboxylate group is clearly protonated, while two other peaks on WAT1004 show the possible positions of hydrogen atoms. (D) Hydrogen bonds observed between the enzyme and the transition-state analogue. Selected residues and atoms on compound **1** are labeled. The hydrogen-bond interactions are represented in dashed lines (see distances in Table 3).

We believe that the boronic acid mimics the acylation transition state on the basis of the geometry it adopts in the site, which closely resembles that of a phosphonate inhibitor bound to the analogous class A β-lactamase, PC1.[49,50] This phosphonate structure was thought to represent the acylation high-energy intermediate geometry.[49] Correspondingly, the position of the boronic acid group differs considerably from that adopted by another boronic acid bound to TEM-1, which was thought to represent the structure of the deacylation high-energy intermediate.[2,3] In the geometry observed here, the O1 oxygen of the boronic acid corresponds to the position of the former lactam carbonyl oxygen in the "oxyanion"[47] or "electrophilic"[48] hole. The hydrogen bond that appears to be likely between the carbonyl oxygen of Ala237 and the O1 boronic oxygen is consistent with the ability of this site to bind to protonated groups, such as hydroxyls, protonated acids, and waters. The O2 boronic oxygen corresponds to the position of the former lactam nitrogen, the leaving group in the acylation reaction. In the 0.85 Å structure, this proxy for the ring nitrogen may donate a proton to Wat1076 and accepts a proton from Ser130 (Figure 4B). Such a pattern would suggest that Ser130 is playing the role of the catalytic acid in the reaction, activating the leaving group, as has been previously suggested.[20,51]

Several aspects of this 0.85 Å resolution structure will interest the specialist. The ultrahigh resolution afforded us experimental evidence for positions of more than 70% of the protons on the protein. These positions are, of course, very important to know when modeling such things as catalytic activity and inhibition from a protein structure, but for many groups on a protein they are rarely observed and must instead be predicted. It may be interesting to compare the proton positions that we observe with those that would have been predicted by widely used prediction programs. These positions may be of direct interest to investigators interested in designing new inhibitors for TEM-1.[2,52,53]

The ultrahigh resolution also affords a view of protein motion that is not typically available in crystal structures. The active site, which is stabilized by a transition state analogue,[19,34,54] appears to be quieter than the rest of the enzyme (Figure 5A). Some motions, such as those observed with the region around residues 212−220, which appears to move as a group, may speak to fluctuation modes experienced by proteins that are relevant to activity.[55,56] Other residues appear to sample side-chain rotamers, relatively independent of other side chains. For

(49) Chen, C. C.; Rahil, J.; Pratt, R. F.; Herzberg, O. *J. Mol. Biol.* **1993**, *234*, 165−78.
(50) Rahil, J.; Pratt, R. F. *Biochem. J.* **1993**, *296*, 389−93.
(51) Atanasov, B. P.; Mustafi, D.; Makinen, M. W. *Proc. Natl. Acad. Sci. U.S.A.* **2000**, *97*, 3160−5.
(52) Strynadka, N. C.; Eisenstein, M.; Katchalski-Katzir, E.; Shoichet, B. K.; Kuntz, I. D.; Abagyan, R.; Totrov, M.; Janin, J.; Cherfils, J.; Zimmerman, F.; Olson, A.; Duncan, B.; Rao, M.; Jackson, R.; Sternberg, M.; James, M. N. *Nat. Struct. Biol.* **1996**, *3*, 233−9.
(53) Rahil, J.; Pratt, R. F. *Biochem. J.* **1991**, *275*, 793−5.
(54) Beadle, B. M.; McGovern, S. L.; Patera, A.; Shoichet, B. K. *Protein Sci.* **1999**, *8*, 1816−24.
(55) Lau, E. Y.; Bruice, T. C. *J. Mol. Biol.* **1999**, *293*, 9−18.
(56) Li, L.; Falzone, C. J.; Wright, P. E.; Benkovic, S. J. *Biochemistry* **1992**, *31*, 7826−33.
(57) Koradi, R.; Billeter, M.; Wuthrich, K. *J. Mol. Graphics* **1996**, *14*, 51−5, 29−32.

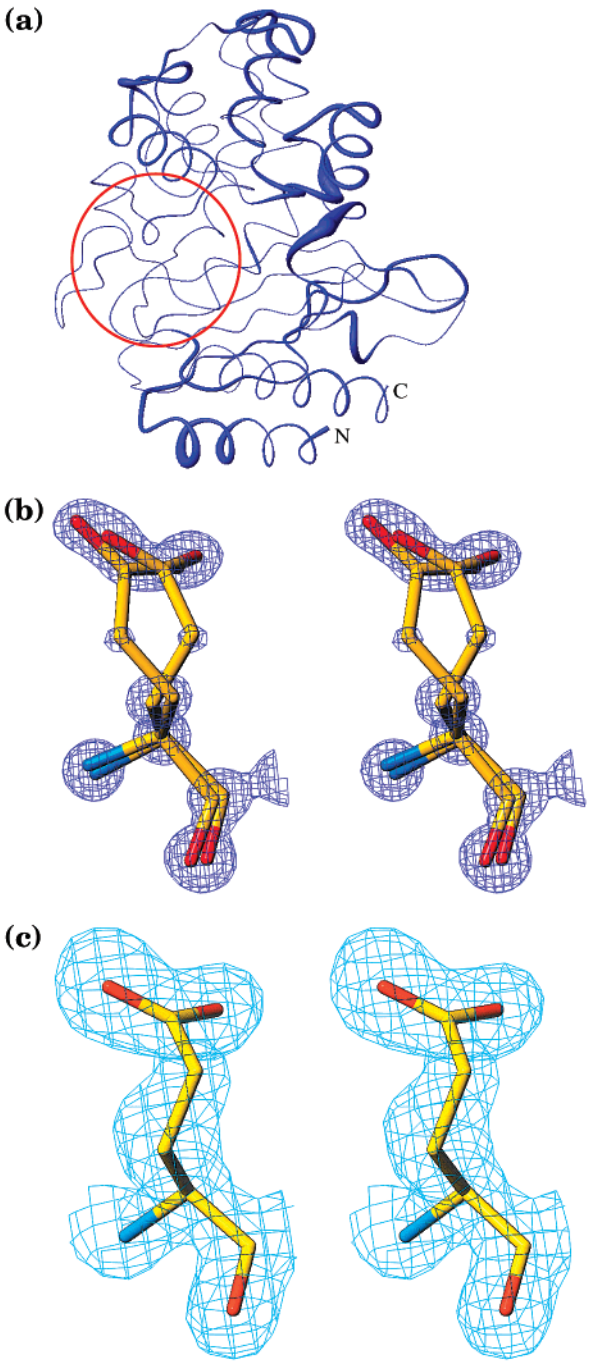

Figure 5. Features of the ultrahigh-resolution structure. (A) The flexibility of TEM M182T complex with compound **1**. The line thickness represents the rmsd of all Cα atoms, using MOLMOL.[57] The N and C termini are labeled, and the active site is circled. (B) Stereoview of two alternative conformers of the Glu58 surrounded with $2F_o - F_c$ σ_A-weighted density map at 2.0σ; both conformers are in low-energy conformations. (C) The same residue in a lower resolution (1.73 Å) crystal structure (PDB code 1JVJ[34]) surrounded with $2F_o - F_c$ density map at 1.0σ. The side chain is well fitted in the density map, but it is in a high-energy conformation.

these residues, the structure sometimes reveals multiple conformations where, at lower resolution, only a single conformation was modeled. An example of this may be seen for Glu58 (Figure 5B and C), which at lower resolution (1.73 Å) was fit as though it were in a single, apparently high-energy conformation.[34] At 0.85 Å resolution, it is clear that this residue is sampling two low-energy conformations that were masked in the lower resolution structure. In this ultrahigh resolution structure, we observe 64% of all residues to occupy more than one conformation, which would suggest that in structures of lower resolution one is fitting only one out of several possible conformations or, occasionally, averaging several conformations together.

Conclusion

The observation of a protonated Glu166 at 0.85 Å resolution, and the hydrogen-bonding network in which it participates, is consistent with this residue acting as the catalytic base in the acylation reaction mechanism. According to such a mechanism, Glu166 would activate Wat1004, which, in turn, would activate Ser70, accepting the proton of the Ser70 nucleophile during the attack on the lactam carbonyl center (Figure 2B). In the transition-state analogue complex structure reported here, the proton has been shuttled from the serine through the water to end up on the glutamic acid. Meanwhile, the leaving group lactam nitrogen (mimicked by O2 of boronic acid) is activated by accepting a proton from Ser130, whose proton is also visible in this structure, hydrogen bonding to the boronic acid O2 (Figure 4B), which acts as a proxy for the lactam nitrogen. The role of Lys73, which in our structure and in previous structures hydrogen bonds with both Ser70 and Ser130,[2] may be to activate both residues electrostatically. Lys73 may also act to transfer a proton to replace the one Ser130 has donated in activating the lactam nitrogen. Such a proton transfer might be essential for an efficient deprotonation of Glu166 for deacylation. Lys73 is optimally positioned to function in such a proton transfer, which can be accommodated to the observation that mutants at Lys73 disrupt enzyme activity, since such mutants would be expected to be less activated if a protonated Glu166 persists. We note that the possibility that Lys73 is acting as the catalytic base (Figure 2C) is not directly falsified by this structure; rather, such a mechanism would now have to bear the additional burden of explaining why Glu166 should be protonated in the acylation high-energy intermediate, and why it should participate in a hydrogen-bonding network that extends to the nucleophilic serine.

Taken together with the NMR pK_a measurement of Lys73,[10] this structure suggests that Glu166 is the most likely candidate for the general base role in acylation, acting through a conserved water. The same water later attacks Ser70 Oγ to release the product with activation again by Glu166, which would make the reaction cycle of class A β-lactamase symmetrical, similar to serine proteases. The high resolution of this structure affords an unusually detailed view of the proton positions on the enzyme overall, as well as some of the ranges of motion that the enzyme experiences. The structure may find broad use for investigators interested in predicting proton positions and protein movements, and find particular application among investigators interested in designing novel inhibitors for this key antibiotic resistance enzyme.

Data Deposition. The coordinates have been deposited in the Protein Data Bank (accession code for compound **1**/TEM-1 M182T complex is 1L7U).

Acknowledgment. This work was supported by G.M. 63815 from the NIH. We thank Emilia Caselli and Fabio Prati for compound **1**. We thank W. Anderson for technical advice, and R. Powers, P. Focia, D. Freymann, and S. McGovern for reading

this manuscript. X-ray crystallographic data were collected at the DuPont−Northwestern−Dow Collaborative Access Team (DND-CAT) synchrotron research center at the Advanced Photon Source (APS). DND-CAT is supported by the DuPont Co., the Dow Chemical Co., the National Science Foundation, and the State of Illinois.

JA0259640